British Journal of Cancer www.nature.com/bjc

ARTICLE OPEN

Check for updates

PANTHER: AZD8931, inhibitor of EGFR, ERBB2 and ERBB3 signalling, combined with FOLFIRI: a Phase I/II study to determine the importance of schedule and activity in colorectal cancer

David J. Propper[1,9], Fangfei Gao[2,9], Mark P. Saunders[3], Debashis Sarker[4], John A. Hartley[5], Victoria J. Spanswick[5], Helen L. Lowe[5], Louise D. Hackett[5], Tony T. Ng[1,2,6], Paul R. Barber[2], Gregory E. Weitsman[7], Sarah Pearce[8], Laura White[8], Andre Lopes[8], Sharon Forsyth[8] and Daniel Hochhauser[2]✉

BACKGROUND: Epidermal growth factor receptor (EGFR) is a therapeutic target to which HER2/HER3 activation may contribute resistance. This Phase I/II study examined the toxicity and efficacy of high-dose pulsed AZD8931, an EGFR/HER2/HER3 inhibitor, combined with chemotherapy, in metastatic colorectal cancer (CRC).
METHODS: Treatment-naive patients received 4-day pulses of AZD8931 with irinotecan/5-FU (FOLFIRI) in a Phase I/II single-arm trial. Primary endpoint for Phase I was dose limiting toxicity (DLT); for Phase II best overall response. Samples were analysed for pharmacokinetics, EGFR dimers in circulating exosomes and Comet assay quantitating DNA damage.
RESULTS: Eighteen patients received FOLFIRI and AZD8931. At 160 mg bd, 1 patient experienced G3 DLT; 160 mg bd was used for cohort expansion. No grade 5 adverse events (AE) reported. Seven (39%) and 1 (6%) patients experienced grade 3 and grade 4 AEs, respectively. Of 12 patients receiving 160 mg bd, best overall response rate was 25%, median PFS and OS were 8.7 and 21.2 months, respectively. A reduction in circulating HER2/3 dimer in the two responding patients after 12 weeks treatment was observed.
CONCLUSIONS: The combination of pulsed high-dose AZD8931 with FOLFIRI has acceptable toxicity. Further studies of TKI sequencing may establish a role for pulsed use of such agents rather than continuous exposure.
TRIAL REGISTRATION NUMBER: ClinicalTrials.gov number: NCT01862003.

British Journal of Cancer; https://doi.org/10.1038/s41416-022-02015-x

BACKGROUND

Monoclonal antibodies targeting EGFR, either when combined with conventional cytotoxic chemotherapy, or as single agents, produce significant survival prolongation in patients with RAS and BRAF wild type metastatic colorectal cancer (mCRC) [1]. In contrast, small molecules targeting the EGFR pathway, such as gefitinib, have minimal activity as either monotherapy or in combination with chemotherapy [2].

A factor limiting the efficacy of agents targeting the EGFR pathway is the compensatory upregulation of HER2 (Erb-B2) and HER3 (Erb-B3), which can activate bypass pathways and hence mediate resistance. It has been suggested primary or acquired resistance to antibodies targeting EGFR could either be due to HER2 gene amplification or heregulin up-regulation (a HER3 ligand), leading to persistent extracellular signal-regulated kinase signalling and resistance to cetuximab [3, 4]. Preclinical and clinical data have demonstrated HER3 as an escape pathway to EGFR blockade through a compensatory shift to HER3 signalling through the PI3K/AKT pathway [5–7]. AZD8931 is a novel tyrosine kinase inhibitor with equipotent inhibition against EGFR, HER2, and HER3 signalling. AZD8931 provides the opportunity to investigate whether simultaneous inhibition of three ERBB receptor pathways could be of benefit in CRC. In the multicentre randomised Phase II/III FOCUS4-D trial, 32 patients with metastatic colorectal cancers WT for BRAF, PIK3Ca, KRAS and NRAS after first line induction therapy were randomised 1:1 to either AZD8931 40 mg bd continuous dosing regimen vs placebo. There was no PFS benefit of AZD8931 compared to placebo [8]. In a Phase I dose escalation study combining AZD8931 with oxaliplatin and capecitabine chemotherapy in oesophagogastric cancer (DEBIOC), AZD8931 dosing of 20 mg bd 4 days on/3 days off demonstrated an acceptable safety profile in patients.

[1]Barts Cancer Institute, Queen Mary, University of London, John Vane Science Centre, Charterhouse Square, London EC1M 6BQ, UK. [2]UCL Cancer Institute, Paul O'Gorman Building, University College London, London WC1E 6DD, UK. [3]The Christie, Manchester M20 4BX, UK. [4]School of Cancer and Pharmaceutical Sciences, King's College London, London WC2R 2LS, UK. [5]UCL ECMC GCLP Facility, UCL Cancer Institute, Paul O'Gorman Building, University College London, London WC1E 6DD, UK. [6]Breast Cancer Now Research Unit, Department of Research Oncology, Guy's Hospital, King's College London, London SE1 9RT, UK. [7]Richard Dimbleby Laboratory of Cancer Research, School of Cancer & Pharmaceutical Sciences, King's College London, London SE1 1UL, UK. [8]Cancer Research UK & UCL Cancer Trials Centre, University College London, London W1T 4TJ, UK. [9]These authors contributed equally: David J. Propper, Fangfei Gao. ✉email: d.hochhauser@ucl.ac.uk

Received: 19 May 2022 Revised: 29 September 2022 Accepted: 4 October 2022
Published online: 09 November 2022

Published on Behalf of CRUK

Both oxaliplatin and irinotecan have shown synergistic activity with AZD8931 in a variety of preclinical models (AstraZeneca, unpublished data). In this trial AZD8931 was assessed in combination with FOLFIRI (irinotecan/5-FU) chemotherapy. This was based on results of Phase III studies in CRC, indicating that cetuximab confers a survival advantage with this regimen [9, 10]. In contrast, two randomised studies using oxaliplatin based chemotherapy with EGFR inhibition (COIN and NORDIC) showed no advantage [9, 11]. There is evidence that in some indications the combination of oxaliplatin with cetuximab could be deleterious with regard to overall survival (OS) [12]. The reasons for this are unclear but may include effects of EGFR inhibition on free radical formation that mediates the cytotoxicity of platinum-based chemotherapy [13].

There is extensive evidence that antibodies targeting EGFR have activity only in tumours expressing wild-type RAS [14–16]. Preclinical data suggest that AZD8931 may have activity in KRAS mutant backgrounds but this is as yet unclear. It was therefore appropriate in this trial to enrol patients with RAS wild-type tumours.

An important issue in determining the efficacy of EGFR inhibition in CRC has been the schedule used. Continuous treatment with TKIs such as gefitinib and erlotinib can result in G1 arrest, which may reduce the effectiveness of agents that are S phase specific such as irinotecan [17]. In contrast, use of high doses of these agents for shorter duration (pulse treatment) inhibit critical downstream signalling pathways without inducing cell cycle arrest [18, 19]. In this study, therefore, we sought evidence of efficacy for pulsed high dose AZD8931 in combination with FOLFIRI in chemotherapy-naive patients with CRC. In addition, we assessed effects of increasing doses of AZD8931 on DNA damage by the single-cell gel electrophoresis (Comet) assay.

The expression level of HER family members is unreliable as a predictive marker for targeted therapies in cancer [5, 20, 21]. HER receptors are able to form alternative dimers and can therefore compensate the loss of function of one receptor during targeted therapies [22, 23]. The HER dimerisation status may therefore be more important than HER receptor expression in determining sensitivity or resistance to therapy [24, 25]. Therefore, the ability to assess the dimerisation receptor pairs within tumours could be useful as a prognostic or predictive biomarker for targeted therapies in metastatic colorectal cancer.

Förster resonance energy transfer (FRET) assays using fluorescence lifetime imaging microscopy (FLIM) have been developed to analyse the interaction between pairs of molecules [26]. This is a gold standard technique for measuring protein proximity within <10 nm range [27]. Fluorescence lifetime imaging (FLIM) is well suited to the analysis of interaction within HER family receptors in cells and FFPE tissues. Using FLIM, it is possible to measure FRET to quantify interactions between HER receptors at nanometre scale to establish the potential role that crosstalk might play in metastatic colorectal cancer. Such data could help characterise or predict response to anti-HER therapy.

Previous work in our group has shown HER2:HER3 crosstalk was required for endogenous feedback HER3 phosphorylation upon cetuximab treatment in metastatic colorectal cancer cells, and co-treatment with cetuximab and lapatinib can limit this effect [28]. In patients with breast cancer, extent of HER2:HER3 dimer formation in tumour blocks predicted likelihood of metastatic relapse after surgery independently of HER2 expression [24]. Furthermore, subset analysis from the COIN trial [9] showed that in patients treated with chemotherapy plus cetuximab, those with increased HER2:HER3 tumour FRET efficiency had superior PFS [29]. Hence, changes in HER2-3 dimerisation were assessed in this trial using an innovative fluorescence resonance energy transfer (FRET) assay.

This trial examined the toxicity and efficacy profile of pulsed AZD8931 in combination with chemotherapy in first-line treatment of RAS WT metastatic colorectal cancer patients and explored potential biomarkers that may predict response to therapy.

METHODS

Participants and study design

Eligible patients with histologically confirmed non-resectable metastatic RAS wild-type metastatic colorectal cancer, and WHO performance status 0–1 were recruited onto this study. Patients were chemotherapy naive for metastatic disease and had RECIST measurable tumours. Prior adjuvant chemotherapy was allowed provided it was completed at least 6 months before trial entry. Patients received oral AZD8931 on days 1–4 in a 2-weekly schedule plus FOLFIRI starting on day 1, given every 2 weeks. Patients remained on treatment until disease progression, unless there were intolerable side-effects, treatment delays longer than 3 weeks or withdrawal of consent. If AZD8931 was stopped patients were permitted to continue to receive FOLFIRI alone.

PANTHER adopted a seamless Phase I/II trial design. Phase I design was done using a dose-escalation continual reassessment method (CRM) [30], which was used to evaluate tolerability of FOLFIRI in combination with AZD8931 20 mg bd, 40 mg bd, 80 mg bd and 160 mg bd, using a target probability of toxicity of 33%. A minimum of two patients were required for a dose escalation decision by the Trial Management Group (TMG). The Phase II part of the trial opened as a randomised trial in July 2016 aiming to recruit 40 patients (20 in each arm), which was sufficient to detect, with an 80% power and 1-sided significance level, an assumed 20% difference in the mean percentage change in the tumour size at 12 weeks from baseline between treatment groups with a standard deviation of 30%. Due to projected expiry of the AZD8931 drug supply, the trial was amended in May 2017 to a single-arm single-stage study aiming to recruit a total of 21 patients to evaluate whether the response rate with AZD8931 was improved by 20% from an assumed historical control response rate of 35%, based on an 80% power and a one-sided alpha of 15%. The requirement for biopsy resulted in significant delays in recruitment for this study.

Outcomes

Dose-limited toxicities including cardiovascular (prolongation of QT interval, congestive cardiac failure or reduction in LVEF) were evaluated from the start of cycle 1 to the end of cycle 2. Disease status was assessed by CT scan and evaluated using RECIST v1.1 at baseline, week 12 and every 12 weeks during treatment. Progression-free survival (PFS) and OS were measured. Adverse events were assessed according to CTCAE v4.03 until 30 days post last trial treatment administration.

Pharmacokinetic and pharmacodynamic studies were carried out as per protocol. Exploratory biological endpoints included analysis of DNA damage and repair by the single-cell gel electrophoresis (Comet) assay in peripheral blood mononuclear cells (PBMCs), profiling of patient serum for ligands including amphiregulin (AR), epidermal growth factor (EGF), heparin-binding EGF (HBEGF) and transforming growth factor alpha (TGF-α) and analysis of circulating exosomes. ERBB dimerisation status was assessed in circulating exosomes.

PBMCs were isolated from patients in Phase I and analysed for the effect of AZD8931 on DNA damage and repair using single-cell gel electrophoresis (Comet) assay [31]. Serum from patients in Phase II were analysed for the presence of AR, EGF, HBEGF and TGF-α biomarkers using the Aushon Ciraplex multiplex ELISA system.

Exosomes from plasma of 13 patients in the Phase I trial, before and after their first dose of AZD8931 were extracted using an in-house optimised ultracentrifugation protocol (Supplementary Methods). Concentration and size distribution of exosome preparations were measured using the Nanosight LM10-HS (Nanosight Ltd, Amesbury, UK), prior to being analysed for proteins of interest including EGFR, HER2, HER3 and S100A9, using dot blot analysis. Exosomal HER2-3 dimers were analysed using FRET/FLIM, and FRET efficiencies was calculated for each patient before and after treatment with AZD8931. FRET score was classified as positive or negative according to whether a significant dimer score could be detected at that patient time point (Supplementary Methods).

Data analysis

Statistical analysis in this study was mostly descriptive. The complete response/partial response (PR) rate was reported along with 70% CI. The change in tumour size at 12 weeks (or time of progression) and adverse events were reported in terms of mean and percentages, respectively. OS and PFS were reported using Kaplan–Meier curves along with median time to event and 12- and 24-month event-free rates. Treatment comparisons in terms of OS and PFS were reported using hazard ratios, 95% confidence interval (CI) and p values (2-sided) derived from Cox regression.

Pharmacokinetic data was described using means between AZD8931 dosing with and without FOLFIRI. 95% CIs were used when appropriate. Marker dot blot change was calculated as percentage change compared to the baseline timepoint 1. FRET class was compared between timepoints. Data analysis was done using STATA 15.1 and R 4.0.

RESULTS

The Phase I part of the trial recruited a total of 13 patients between July 2014 and April 2016 from four hospital sites (Fig. 1). Of those, 12 were evaluable for DLT: 2 patients were treated at each of the 20, 40 and 80 mg bd dose levels and 6

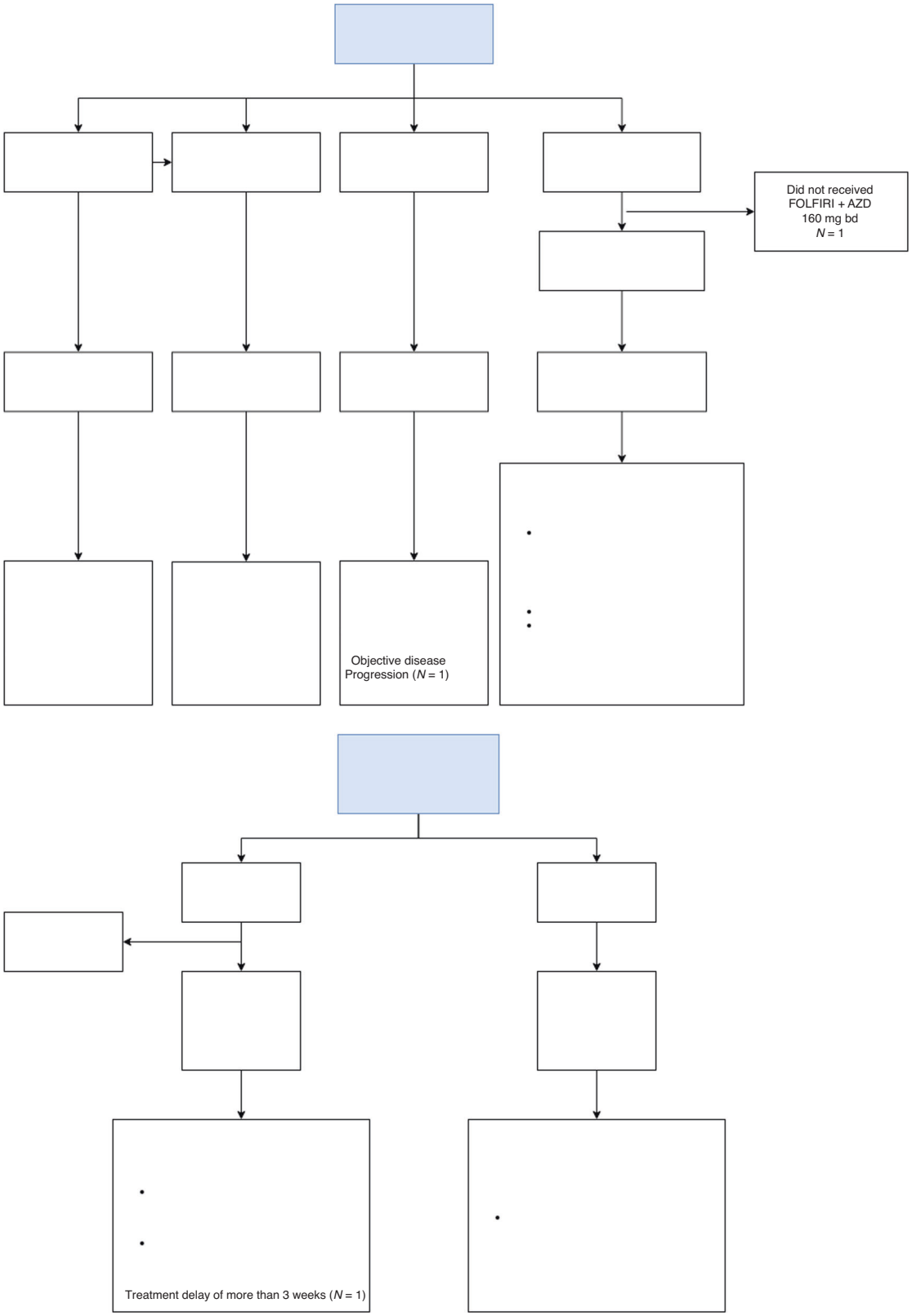

Fig. 1 Study flow chart for Phase I and phase II cohorts.

Table 1. Baseline characteristics.

Baseline characteristics	Any AZD dose $N = 18$ N (%)
Age in years	
Median (range)	63 (37–77)
BMI in kg/m^2	
Median (range)	26 (19–32)
Sex	
Male	15 (83%)
Female	3 (17%)
WHO performance status	
0 (fully active)	13 (72%)
1 (restricted in physical activity)	5 (28%)
Previous surgery	
No	5 (28%)
Yes	13 (72%)
Stent in situ	
No	14 (78%)
Yes	3 (17%)
Unknown	1 (6%)
Previous radiotherapy for localised disease	
No	15 (83%)
Yes	3 (17%)
Previous adjuvant chemotherapy	
No	13 (72%)
Yes	5 (28%)
Previous hormonal/biological/immunological therapy	
No	18 (100%)

patients were treated at the 160 mg bd dose level. A total of 11 patients were recruited into Phase II from 4 sites between September 2016 and June 2017. All 6 patients registered to FOLFIRI and AZD8931 and 4 of the 5 patients allocated to FOLFIRI alone started treatment (1 patient decided to withdraw before start of FOLFIRI). A total of 18 patients (12 in Phase I and 6 in Phase II) received FOLFIRI and AZD8931 and are the evaluable population in this study. Baseline characteristics are outlined in Table 1. All 18 patients had measurable target lesions.

Treatment compliance

The reasons for treatment discontinuation were: progressive disease (PD)—7/18 patients, 39%; adverse events related to treatment (AZD8931 and/or FOLFIRI) - 4/18, 22%; (2 diarrhoea, 1 skin reaction, 1 febrile neutropenia); treatment delay of more than 3 weeks due to unrelated reasons - 4/18, 22%, patient choice - 2/18, 11% and adverse events not related to treatment - 1/18, 6%.

Toxicity and safety

Only 1 patient receiving AZD8931 160 mg bd experienced a grade 3 DLT (papulopustular rash), establishing the AZD8931 160 mg bd as the recommended dose to be tested in the cohort expansion. There were no grade 5 adverse events. A total of 13 (72%) patients had at least a grade 3 adverse event. Of those, 4 (22%) had a grade 4 adverse event: 1 patient received AZD8931 80 mg bd and had sepsis and thromboembolic event; 1 patient had colonic perforation and 2 patients had sepsis in the AZD8931 160 mg bd arm. The most common grade 3 events among patients who received AZD8931 and FOLFIRI were diarrhoea (4, 33%), neutrophil count decreased (4, 33%), hypertension (3, 25%) and GGT increased (3, 25%). Table 2 presents the reported adverse events related to AZD8931.

Response of patients on study

Table 3 shows the best overall response rate by cohort.

The best overall response rate among the 18 patients treated with AZD8931 is 33% (exact 95% CI: 13–59%, 70% CI: 21–48%). The best overall response rate among the 12 patients treated with AZD8931 at 160 mg bd is 25% (exact 95% CI: 5–57%, 70% CI: 11–44%). Based on the estimated rate and on the estimated 70% CI, there is no evidence, at 1-sided 15% significance level, that the response rate among those who received AZD8931 160 mg bd (from Phase I and Phase II) was higher than the assumed response rate of 35% in historical controls.

The mean % change in the sum of longest diameters at 12 weeks from baseline among all 18 patients who received AZD8931 was −10.02% (95% CI: −22.97 to 2.92) and among the 12 patients who received 160 mg bd was −7.60% (95% CI −21.82 to 6.62). One patient who received 160 mg bd had a 21% shrinkage in target lesions at 12 weeks but also had new lesions identified and was therefore assessed as having progressive disease.

Time-to-event outcomes

The median follow-up time among the 18 patients registered who received AZD8931 is 32.2 months. Figure 2 shows key information about time-to-event outcomes.

A total of 17 (94%) patients had a reported PFS event (progression or death) and 12 (67%) deaths have been reported. The cause of death was disease progression for 6 patients, 2 due to sepsis, 1 pneumonia and 3 due to other unknown reasons. Figure 3 presents the PFS and OS curves among the 12 patients who received 160 mg bd AZD8931.

Among this group, the median PFS time was 8.7 months, and the 12 and 24 months PFS rate was 25% (6–50%) and 17% (3–41%), respectively; the median OS was 21.2 months, and the 12- and 24-month OS rate 67% (34–86%) and 50% (21–74%), respectively. Patients who received any AZD dose presented improved OS when compared to patients who received FOLFIRI alone (Supplementary Fig. 1A, HR: 0.23 (95% CI: 0.06–0.84), $p = 0.03$) but PFS was similar between these two groups (Supplementary Fig. 1B, 0.81 (95% CI: 0.27–2.49), $p = 0.72$).

Pharmacokinetics

Plasma was isolated from whole blood collected pre-treatment and at 1.5, 2.5, 4, 8, 10 and 24 h post-FOLFIRI infusion, at cycle 1 day and cycle 3 day 1. The mean AUC (0-t) for AZD8931 at 20 mg bd was 11,395.5 and 12,493.78 ng/mL, at 40 mg bd was 20,795.4 and 22,864 ng/mL, at 80 mg bd was 55,156.75 and 72,049.15 ng/mL and at 160 mg bd was 137,221.39 and 185,184.96 ng/mL, when AZD8931 was administered without and with FOLFIRI, respectively. The mean AUC (0–*t*) for irinotecan when administered without and with AZD8931 was not substantially different across dose levels (598.5 vs 511.7 µg/mL at 20 mg bd; 547.8 vs 537.2 µg/mL at 40 mg bd, 765.0 vs 774.7 µg/mL at 80 mg bd; and 716.1 vs 750.0 µg/mL at 160 mg bd). Similar patterns were observed for the other PK parameters. Therefore, combination treatment did not alter pharmacokinetics of either AZD8931 or irinotecan.

Pharmacodynamic analysis

No significant difference was observed in DNA damage as measured as Olive tail moment (OTM) (µm) between patient dose cohorts of AZD8931 (Supplementary Fig. 2).

Table 2. Adverse events reported as related to AZD8931 by grade.

Adverse events reported as related to AZD8931 (worst grade per patient)	Any AZD dose level			
	N = 18			
	N (%)			
	Grade 1	Grade 2	Grade 3	Grade 4
Blood and lymphatic system disorders				
Anaemia	1 (6%)	2 (11%)	–	–
Febrile neutropenia	–	–	1 (6%)	–
Other blood and lymphatic system disorders	1 (6%)	–	–	–
Eye disorders				
Blurred vision	3 (17%)	–	–	–
Dry eye	2 (11%)	–	–	–
Eye pain	1 (6%)	–	–	–
Other eye disorders	1 (6%)	–	–	–
Gastrointestinal disorders				
Abdominal pain	2 (11%)	–	–	–
Constipation	4 (22%)	–	–	–
Diarrhoea	7 (39%)	–	4 (22%)	–
Dry mouth	1 (6%)	–	–	–
Dyspepsia	1 (6%)	–	–	–
Flatulence	2 (11%)	–	–	–
Gastro-oesophageal reflux disease	2 (11%)	–	–	–
Mucositis oral	3 (17%)	2 (11%)	1 (6%)	–
Nausea	6 (33%)	3 (17%)	–	–
Oral pain	1 (6%)	–	–	–
Other gastrointestinal disorders	1 (6%)	–	–	–
Vomiting	1 (6%)	–	–	–
General disorders and administration site conditions				
Chills	1 (6%)	–	–	–
Fatigue	7 (39%)	8 (44%)	1 (6%)	–
Fever	–	1 (6%)	–	–
Flu-like symptoms	2 (11%)	–	–	–
Infections and infestations				
Lip infection	1 (6%)	–	–	–
Papulopustular rash	3 (17%)	1 (6%)	1 (6%)[a]	–
Paronychia	1 (6%)	–	–	–
Sepsis	–	–	–	1 (6%)
Investigations				
Neutrophil count decreased	–	–	3 (17%)	–
Other Investigations	2 (11%)	–	–	–
Weight loss	–	1 (6%)	–	–
Metabolism and nutrition disorders				
Anorexia	5 (28%)	1 (6%)	–	–
Nervous system disorders				
Concentration impairment	1 (6%)	–	–	–
Dysgeusia	3 (17%)	–	–	–
Headache	1 (6%)	–	–	–
Lethargy	1 (6%)	–	–	–
Movements involuntary	1 (6%)	–	–	–
Renal and urinary disorders				
Cystitis noninfective	1 (6%)	–	–	–

Table 2. continued

Adverse events reported as related to AZD8931 (worst grade per patient)	Any AZD dose level			
	N = 18			
	N (%)			
	Grade 1	Grade 2	Grade 3	Grade 4
Respiratory, thoracic and mediastinal disorders				
Dyspnoea	–	1 (6%)	–	–
Epistaxis	2 (11%)	–	–	–
Hiccups	1 (6%)	–	–	–
Hoarseness	1 (6%)	–	–	–
Other respiratory, thoracic and mediastinal disorders	1 (6%)	–	–	–
Skin and subcutaneous tissue disorders				
Alopecia	2 (11%)	–	–	–
Dry skin	8 (44%)	–	–	–
Nail loss	1 (6%)	–	–	–
Other skin and subcutaneous tissue disorders	1 (6%)	–	–	–
Pain of skin	1 (6%)	–	–	–
Palmar–plantar erythrodysesthesia syndrome	1 (6%)	–	–	–
Periorbital oedema	1 (6%)	–	–	–
Pruritus	1 (6%)	–	–	–
Rash acneiform	7 (39%)	1 (6%)	–	–
Rash maculo-papular	2 (11%)	–	–	–
Scalp pain	2 (11%)	–	–	–
Vascular disorders				
Thromboembolic event	–	1 (6%)	1 (6%)	1 (6%)
Number of patients experiencing any adverse event				
Any adverse event	4 (22%)	6 (33%)	7 (39%)	1 (6%)

Note: The numbers represent the count (%) of patients experiencing an adverse reaction based on their worst grade. The same patient can be counted across multiple rows because a patient can experience multiple events.
[a]Dose-limiting toxicity.

Table 3. Best overall response.

Best overall response	FOLFIRI and AZD8931			
	AZD 20 mg bd	AZD 40 mg bd	AZD 80 mg bd	AZD 160 mg bd
	N = 2	*N* = 2	*N* = 2	*N* = 12
	N (%)	*N* (%)	*N* (%)	*N* (%)
Partial response	1 (50%)	1 (50%)	1 (50%)	3 (25%)
Stable disease	–	1 (50%)	–	8 (67%)
Progressive disease	1 (50%)	–	–	1 (8%)
Not assessed	–	–	1 (50%)[a]	–

[a]Patient died prior to 12-week scan.

Ligand analysis was performed on a total of 22 samples received for 9 patients but due to the small numbers it is not possible to present any results or conclusions to this.

Exosomal protein and HER 2-3 dimer analysis

Exosomes from plasma of 13 patients before and after their first dose of AZD8931 were extracted and analysed for proteins of interest and HER2-3 dimer quantity. Plasma-derived exosomes were characterised by the presence of exosome surface marker proteins CD63 and ALIX. HER proteins were consistently detected from circulating exosomes and their quantities changed with treatment (Supplementary Fig. 3). Treatment induced changes in FRET dimer scores were also determined and patients were classified as FRET positive or negative according to the raw FRET efficiency values (Table 4 and Supplementary Fig. 4).

We observed changes in HER markers (Table 5) and FRET dimer scores (Table 4) between time points 1 and 3.

Two patients of the three who had a PR at 12 weeks had a decreased HER2-3 dimer score between those time points; no other patients showed this response. The one patient who had PD at 12 weeks had an increased HER2-3 dimer score and a decreased EGFR/HER-3; again no other patient had this response. All other

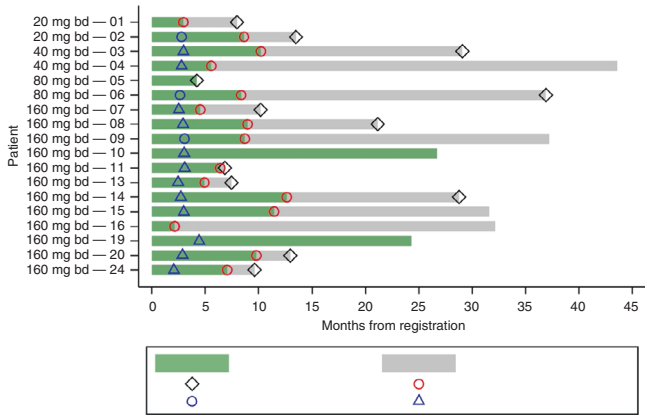

Fig. 2 Swimmer plot of 18 AZD8931-treated patients. The swimmer plot depicts individual patient responses at 12 weeks, duration until disease progression, and duration until death or last follow-up.

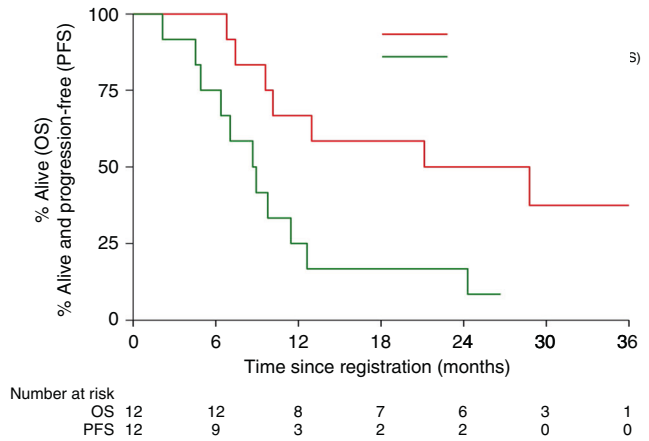

Fig. 3 Kaplan-Meier for progression-free survival (PFS) and for overall survival (OS) among patients who received FOLFORI and AZD8931 160 mg bd. PFS events were defined as disease progression or death, whichever occurred first. OS events include deaths from any cause. Number at risk are given under the plot.

patients had stable disease at 12 weeks and experienced no change in any dimer score.

DISCUSSION

This study showed that the administration of pulse high-dose AZD8931 160 mg bd was well tolerated being associated with a relatively low toxicity profile. However, the best overall response rate among the patients treated with AZD8931 160 mg bd was 25% (all PRs) and therefore it was not shown to be improved when compared to the assumed historical control rate of 35%.

Preclinical studies show that EGFR inhibition enhances responses to DNA-interactive chemotherapies by a variety of mechanisms including inhibition of DNA repair [32]. However, the use of small molecules to inhibit the EGFR pathway has had limited success. A Phase II trial of gefitinib in combination with chemotherapy resulted in responses in a significant proportion of patients but drug-induced toxicities including rash and diarrhoea prevented further development of this strategy [33].

A potentially important factor in the lack of success in these combinations may be the cell cycle effects of TKI treatment of cancers. Gefitinib induces a cell cycle arrest in G1 phase with chronic administration and this may inhibit the effects of agents which act preferentially in S phase such as irinotecan. For example, in a preclinical study in breast cancer of the effects of gefitinib, short-term administration was associated with enhanced DNA damage when combined with DNA-interactive chemotherapies, whereas chronic exposure of cells for 48 h resulted in G1 arrest and diminished efficacy of the combination [34]. The current trial using pulsed high doses of AZD8931 immediately prior and early during cytotoxic chemotherapy was designed to minimise effects on cell cycle distribution of cancer cells.

From the limited and preliminary data in this study, there is no evidence that AZD8931 improves the rate of response when compared with historical control data. However, these preliminary data suggest that giving AZD8931 in combination with FOLFIRI is feasible and tolerable. In the FOCUS4-D study of metastatic colorectal cancer, patients with tumours that were stable or responding to cytotoxic chemotherapy received single agent AZD8931 40 mg bd continuously, and there was no PFS benefit of AZD8931 compared with placebo [8]. Despite using doses that were between 4 and 8 times higher than those previously used, the toxicity attributed to AZD8931 in this study was lower than that reported in studies using more prolonged dosing schedules

Table 4. Dimer score changes before and after first dose of AZD8931.

Patient number	HER1:HER3		HER2:HER3		Response at 12 weeks
	Baseline	After AZD8931	Baseline	After AZD8931	
1	Positive	Negative	Negative	Positive	PD
2	Negative	Negative	Positive	Negative	PR
3	–	–	Negative	Negative	SD
4	–	–	Negative	Negative	SD
5	Negative	Negative	Negative	Negative	–
6	Negative	Negative	Positive	Negative	PR
7	–	–	Positive	Positive	SD
8	–	–	Negative	Negative	SD
9	Negative	Negative	Negative	Negative	PR
10	Negative	Negative	–	–	SD
11	Negative	Positive	Negative	Negative	SD
12	–	–	–	–	–
13	Negative	Negative	–	–	SD

Table 5. Protein expression changes before and after first dose of AZD8931.

Patient number	S100		HER1		HER2		HER3		Response at 12 weeks
	Baseline	% change after AZD8931	Baseline	% change after AZD8931	Baseline	% change after AZD8931	Baseline	% change after AZD8931	
1	1.10	−9.90	0.96	−31.00	0.92	−24.00	0.92	73.00	PD
2	1.30	12.00	0.51	12.00	1.10	33.00	1.10	13.00	PR
3	0.82	−7.00	0.99	−2.40	1.40	−22.00	1.40	−50.00	SD
4	1.10	−13.00	0.47	−34.00	0.78	−15.00	0.78	−30.00	SD
5	0.79	19.00	1.90	−14.00	1.10	−8.00	1.10	−89.00	–
6	–	–	–	–	–	–	–	–	PR
7	0.66	–	0.39	–	0.77	–	0.77	–	SD
8	0.54	3.60	0.78	−35.00	0.87	−15.00	0.87	−41.00	SD
9	–	–	–	–	–	–	–	–	PR
10	1.40	−6.10	0.69	−14.00	0.87	66.00	0.87	68.00	SD
11	2.10	–	1.00	–	1.20	–	1.20	–	SD
12	–	–	–	–	–	–	–	–	–
13	0.94	–	0.48	–	1.30	–	1.30	–	SD

and was in general well-tolerated [8, 35]. Thus, high-dose pulse scheduling in combination with standard doses of cytotoxic chemotherapy appears feasible.

Although there have been many studies investigating inhibition of EGFR in CRC little is known regarding the dynamics of the EGFR pathway in human cancers. We have previously demonstrated that the combined use of HER2-HER3 dimer imaging (applied to FFPE pathological specimens) and conventional mutation analyses can identify in a predictive manner the small subclass of metastatic CRC patients (15%) who will have better prognosis following chemotherapy/cetuximab treatment [29]. One hypothesis is that low affinity EGFR ligands amphiregulin (AREG) and epiregulin (EREG) which are positively predictive of anti-EGFR treatment outcome, may induce prolonged and more widespread signalling, involving the formation of non-EGFR heterodimers such as HER2-3 [36, 37]. In colorectal cell lines, we observed that treatment with AZD8931 resulted in increased HER2-3 dimer formation in cetuximab-sensitive cell line LIM1215 and reduced HER2-3 dimer formation in DLD1 (KRAS WT) (Supplementary Fig. 5). Previous work in our group also demonstrated, for the first time, increased HER2-3 dimerisation upon cetuximab treatment in colon cancer cells [28].

In this study, we observed both increase and decrease of HER 2-3 dimer formation in patients after treatment with AZD8931, correlating to findings in cell line data. Our group have previously reported in breast cancer HER2-3 dimer quantification in formalin-fixed paraffin-embedded (FFPE) tumours predicted metastatic relapse post-surgery that was independent of HER2 expression [24]. The significance of these findings will need to be explored in future colorectal cancer trials using different HER2 targeted agents.

In the literature, there is a presumption that pan-HER tyrosine kinase inhibitors reduce the formation of homologous/heterodimer of HER receptors [38]. Our results indicate HER2-3 heterodimers measured in blood exosomes can increase or decrease following treatment and our preliminary results indicate that the relationship between this dynamic response and tumour response as assessed by RECIST should be further defined in patients with metastatic colorectal cancer treated with anti-HER therapies. It seems likely that inhibition of multiple members of the HER family will have additional biological effects as compared with EGFR alone. The current study included only a limited number of patients and hence no definitive conclusions can be made regarding the utility of this combination approach. Future studies incorporating combinations of chemotherapy and targeted agents should include measurement of translational endpoints which assess pathway activation.

CONCLUSION

This study established that a 4-day pulsed high dose schedule AZD8931 of 160 mg bd is safe and sufficiently tolerated when combined with FOLFIRI. Further studies of TKI sequencing may establish a role for pulsed use of such agents rather than continuous exposure.

DATA AVAILABILITY

Data will be available for sharing after the main trial publication is released. All requests for data will be considered by the Chief Investigator/TMG and, if approved, shared via a data sharing agreement. Decision making factors will include: Data use is in keeping with patient consent. Confidentiality is maintained at all times i.e. no patient identifiable data, such as date of birth will be provided. Data are appropriate for intended purpose. Compliance with legal and ethical requirements is maintained.

CODE AVAILABILITY

The code used for data cleaning and analysis is available upon request from ctc.panther@ucl.ac.uk.

REFERENCES

1. Van Cutsem E, Cervantes A, Adam R, Sobrero A, Van Krieken JH, Aderka D, et al. ESMO consensus guidelines for the management of patients with metastatic colorectal cancer. Ann Oncol. 2016;27:1386–422.
2. Kindler HL, Friberg G, Skoog L, Wade-Oliver K, Vokes EE. Phase I/II trial of gefitinib and oxaliplatin in patients with advanced colorectal cancer. Am J Clin Oncol. 2005;28:340–4.
3. Bardelli A, Jänne PA. The road to resistance: EGFR mutation and cetuximab. Nat Med. 2012;18:199–200.
4. Yonesaka K, Zejnullahu K, Okamoto I, Satoh T, Cappuzzo F, Souglakos J, et al. Activation of ERBB2 signaling causes resistance to the EGFR-directed therapeutic antibody cetuximab. Sci Transl Med. 2011;3:99ra86.
5. Scartozzi M, Mandolesi A, Giampieri R, Bittoni A, Pierantoni C, Zaniboni A, et al. The role of HER-3 expression in the prediction of clinical outcome for advanced colorectal cancer patients receiving irinotecan and cetuximab. Oncologist. 2011;16:53–60.
6. Sergina NV, Rausch M, Wang D, Blair J, Hann B, Shokat KM, et al. Escape from HER-family tyrosine kinase inhibitor therapy by the kinase-inactive HER3. Nature. 2007;445:437–41.

7. Wheeler DL, Huang S, Kruser TJ, Nechrebecki MM, Armstrong EA, Benavente S, et al. Mechanisms of acquired resistance to cetuximab: role of HER (ErbB) family members. Oncogene. 2008;27:3944–56.
8. Adams R, Brown E, Brown L, Butler R, Falk S, Fisher D, et al. Inhibition of EGFR, HER2, and HER3 signalling in patients with colorectal cancer wild-type for BRAF, PIK3CA, KRAS, and NRAS (FOCUS4-D): a phase 2–3 randomised trial. Lancet Gastroenterol Hepatol. 2018;3:162–71.
9. Maughan TS, Adams RA, Smith CG, Meade AM, Seymour MT, Wilson RH, et al. Addition of cetuximab to oxaliplatin-based first-line combination chemotherapy for treatment of advanced colorectal cancer: results of the randomised phase 3 MRC COIN trial. Lancet. 2011;377:2103–14.
10. Van Cutsem E, Köhne C, Hitre E, Zaluski J, Chien CC, Makhson A, et al. Cetuximab and chemotherapy as initial treatment for metastatic colorectal cancer. N Engl J Med. 2009;360:1408–17.
11. Tveit KM, Guren T, Glimelius B, Pfeiffer P, Sorbye H, Pyrhonen S, et al. Phase III trial of cetuximab with continuous or intermittent fluorouracil, leucovorin, and oxaliplatin (Nordic FLOX) versus FLOX alone in first-line treatment of metastatic colorectal cancer: the NORDIC-VII study. J Clin Oncol. 2012;30:1755–62.
12. Bridgewater JA, Pugh SA, Maishman T, Eminton Z, Mellor J, Whitehead A, et al. Systemic chemotherapy with or without cetuximab in patients with resectable colorectal liver metastasis (New EPOC): long-term results of a multicentre, randomised, controlled, phase 3 trial. Lancet Oncol. 2020;21:398–411.
13. Santoro V, Jia R, Thompson H, Nijhuis A, Jeffery R, Kiakos K, et al. Role of reactive oxygen species in the abrogation of oxaliplatin activity by cetuximab in colorectal cancer. J Natl Cancer Inst. 2016;108:djv394.
14. Bokemeyer C, Kohne C, Ciardiello F, Lenz H, Heinemann V, Klinkhardt U, et al. Treatment outcome according to tumor *RAS* mutation status in OPUS study patients with metastatic colorectal cancer (mCRC) randomized to FOLFOX4 with/without cetuximab. J Clin Oncol. 2014;32(Suppl 15):abstract 3505.
15. Douillard J, Oliner KS, Siena S, Tabernero J, Burkes R, Barugel M, et al. Panitumumab-FOLFOX4 treatment and RAS mutations in colorectal cancer. N Engl J Med. 2013;369:1023–34.
16. Van Cutsem E, Lenz H, Köhne C, Heinemann V, Tejpar S, Melezínek I, et al. Fluorouracil, leucovorin, and irinotecan plus cetuximab treatment and RAS mutations in colorectal cancer. J Clin Oncol. 2015;33:692–700.
17. Solit DB, She Y, Lobo J, Kris MG, Scher HI, Rosen N, et al. Pulsatile administration of the epidermal growth factor receptor inhibitor gefitinib is significantly more effective than continuous dosing for sensitizing tumors to paclitaxel. Clin Cancer Res. 2005;11:1983–9.
18. Dimco G, Knight RA, Latchman DS, Stephanou A. STAT1 interacts directly with cyclin D1/Cdk4 and mediates cell cycle arrest. Cell Cycle. 2010;9:4638–49.
19. Tang D, Liu CYJ, Shen D, Fan S, Su X, Ye P, et al. Assessment and prognostic analysis of EGFR, HER2, and HER3 protein expression in surgically resected gastric adenocarcinomas. OncoTargets Ther. 2015;8:7–14.
20. Modjtahedi H, Essapen S. Epidermal growth factor receptor inhibitors in cancer treatment: advances, challenges and opportunities. Anticancer Drugs. 2009;20:851–5.
21. Khelwatty SA, Essapen S, Bagwan I, Green M, Seddon AM, Modjtahedi H, et al. Co-expression of HER family members in patients with Dukes' C and D colon cancer and their impacts on patient prognosis and survival. PLoS ONE. 2014;9:e91139.
22. Holbro T, Beerli RR, Maurer F, Koziczak M, Barbas CF, Hynes NE. The ErbB2/ErbB3 heterodimer functions as an oncogenic unit: ErbB2 requires ErbB3 to drive breast tumor cell proliferation. Proc Natl Acad Sci USA. 2003;100:8933–8.
23. Fruhwirth GO, Fernandes LP, Weitsman G, Patel G, Kelleher M, Lawler K, et al. How Förster resonance energy transfer imaging improves the understanding of protein interaction networks in cancer biology. ChemPhysChem. 2011;12:442–61.
24. Weitsman G, Barber PR, Nguyen LK, Lawler K, Patel G, Woodman N, et al. HER2-HER3 dimer quantification by FLIM-FRET predicts breast cancer metastatic relapse independently of HER2 IHC status. Oncotarget. 2016;7:51012–26.
25. Waterhouse BR, Gijsen M, Barber PR, Tullis IDC, Vojnovic B, Kong A. Assessment of EGFR/HER2 dimerization by FRET-FLIM utilizing Alexa-conjugated secondary antibodies in relation to targeted therapies in cancers. Oncotarget. 2011;2:728–36.
26. Kelleher MT, Fruhwirth G, Patel G, Ofo E, Festy F, Barber PB, et al. The potential of optical proteomic technologies to individualize prognosis and guide rational treatment for cancer patients. Target Oncol. 2009;4:235–52.
27. Ng T, Squire S, Hansra G, Bornancin F, Prevostel C, Hanby A, et al. Imaging protein kinase Cα activation in cells. Science. 1999;283:2085–9.
28. Bosch-Vilaró A, Jacobs B, Pomella V, Abbasi Asbagh L, Kirkland R, Michel J, et al. Feedback activation of HER3 attenuates response to EGFR inhibitors in colon cancer cells. Oncotarget. 2017;8:4277–88.
29. Barber PR, Weitsman G, Lawler K, Barrett JE, Rowley M, Rodriguez-Justo M, et al. HER2-HER3 heterodimer quantification by FRET-FLIM and patient subclass analysis of the COIN colorectal trial. J Natl Cancer Inst. 2020;112:944–54.
30. Sweeting MJ, Wheeler GM. bcrm: Bayesian continual reassessment method for phase I dose-escalation trials. R package v0.5.4. 2019. https://cran.r-project.org/web/packages/bcrm/index.html.
31. Hartley JM, Spanswick VJ, Hartley JA. Measurement of DNA damage in individual cells using the single cell gel electrophoresis (Comet) assay. Methods Mol Biol. 2011;731:309–20.
32. Mahajan K, Mahajan NP. Cross talk of tyrosine kinases with the DNA damage signaling pathways. Nucleic Acids Res. 2015;43:10588–601.
33. Fisher GA, Kuo T, Ramsey M, Schwartz E, Rouse RV, Cho CD, et al. A phase II study of gefitinib, 5-fluorouracil, leucovorin, and oxaliplatin in previously untreated patients with metastatic colorectal cancer. Clin Cancer Res. 2008;14:7074–9.
34. Corkery B, Crown J, Clynes M, O'Donovan N. Epidermal growth factor receptor as a potential therapeutic target in triple-negative breast cancer. Ann Oncol. 2009;20:862–7.
35. Thomas A, Virdee PS, Eatock M, Lord SR, Falk S, Anthoney DA, et al. Dual Erb B Inhibition in Oesophago-gastric Cancer (DEBIOC): a phase I dose escalating safety study and randomised dose expansion of AZD8931 in combination with oxaliplatin and capecitabine chemotherapy in patients with oesophagogastric adenocarcinoma. Eur J Cancer. 2020;124:131–41.
36. Freed DM, Bessman NJ, Kiyatkin A, Salazar-Cavazos E, Byrne PO, Moore JO, et al. EGFR ligands differentially stabilize receptor dimers to specify signaling kinetics. Cell. 2017;171:683–95.
37. Komurasaki T, Toyoda H, Uchida D, Morimoto S. Epiregulin binds to epidermal growth factor receptor and ErbB-4 and induces tryosine phosphorylation of epidermal growth factor receptor, ErbB-2, ErbB-3 and ErbB-4. Oncogene. 1997;15:2841–8.
38. Xuhong JC, Qi XW, Zhang Y, Jiang J. Mechanism, safety and efficacy of three tyrosine kinase inhibitors lapatinib, neratinib and pyrotinib in HER2-positive breast cancer. Am J Cancer Res. 2019;9:2103–19.

ACKNOWLEDGEMENTS

The trial was coordinated centrally by Cancer Research UK and UCL Cancer Trials Centre, London.

AUTHOR CONTRIBUTIONS

DP, MS, DS provided clinical management of patients on the trial and helped write the manuscript. FG did the exosome and HER2-3 dimer analyses and helped write the manuscript. JH, VS, HL did the analysis of DNA damage and repair by the Comet assay and helped write the manuscript. LH did the pharmacokinetic analysis. TN supervised the exosome and HER2-3 dimer analysis and helped write the manuscript. PB, GW did the HER2-3 dimer analysis and helped write the manuscript. SP, LW, SLF provided central coordination for the trial and helped write the manuscript. AL provided statistical support for the trial and helped write the manuscript. DH designed the trial, provided clinical management of patients on the trial and helped write the manuscript.

FUNDING

The trial was funded by Cancer Research UK New Agents Committee and AstraZeneca. Free AZD8931 was provided by AstraZeneca. The trial was sponsored by University College London. The funders had no role in the design of this study and did not have any role during its execution, analyses, interpretation of the data, or decision to submit results.

COMPETING INTERESTS

TTN is Chief Medical Officer of Nano Clinical Ltd. PRB has shares in, and is a consultant for, Nano Clinical Ltd. All other authors declare no conflicts of interest.

ETHICS APPROVAL AND CONSENT TO PARTICIPATE

The trial was approved by the National Research Ethics Service Committee: London – Bloomsbury (12/LO/1822), the Medicines and Healthcare Products Regulatory Agency (Clinical Trials Authorisation number 20363/0315/0014-0001), and by the Research and Development department of each participating NHS Trust. The trial was conducted according to the principles of the International Conference on Harmonisation on Good Clinical Practice. All patients gave written informed consent prior to undergoing any trial-specific procedures.

CONSENT FOR PUBLICATION

N/A.

ADDITIONAL INFORMATION

Supplementary information The online version contains supplementary material available at https://doi.org/10.1038/s41416-022-02015-x.

Correspondence and requests for materials should be addressed to Daniel Hochhauser.

Reprints and permission information is available at http://www.nature.com/reprints

Publisher's note Springer Nature remains neutral with regard to jurisdictional claims in published maps and institutional affiliations.

SUPPLEMENTARY MATERIALS

Supplementary Methods

Serum Exosome Isolation

Patients' frozen serum (-80 ºC) was used for exosome isolation using an optimized ultracentrifugation method (Monypenny et al., 2018). Serum samples were thawed on ice, and 500 μl were diluted 1:3 with sterile, 0.45 μm-filtered PBS to make it up to 1.5 ml.

The diluted serum was centrifuged at 300×g for 10 min to remove cell debris, at 5,000×g for 20 min to remove large vesicles and membrane fragments, then at 12,200×g for 30 min to deplete microvesicles (MV), the last step was repeated for an extra 30 min, to prevent any further MV contamination of the exosomal fraction. This was followed by 100,000×g ultracentrifugation for 120 min to pellet exosomes using micro-ultracentrifuge tubes (1.5 ml, Cat No. 357448, Beckman Coulter) in a Beckman Optima-Max XP ultracentrifuge equipped with a TLA-55 rotor (Beckman Coulter). After centrifugation, the supernatant was carefully removed and the pellets washed with sterile PBS. A second 100,000×g ultracentrifugation for 60 min was used and the resulting pellets were resuspended in 100 μl of sterile, 0.45 □m-filtered PBS. All centrifugation steps were performed at 4 °C. From purified exosomal fractions, 5-20 μl were diluted up to 1 ml in PBS and used for nanoparticle tracking analysis (NTA) using a Nanosight LM-14 system (Malvern Ltd) as described previously using constant flow injection. The NTA analysis software was used to calculate the particle population size distribution including the derivation of the population's modal particle diameter.

Peripheral Blood Mononuclear Cell Isolation

Peripheral blood mononuclear cells (PBMCs) were isolated from whole blood, taken from patients at the following time points:-

- Pre-treatment: within 7 days of first dose of AZD8931
- Cycle 1 Day 1: before morning dose of AZD8931 + FOLFIRI administration
- Cycle 1 Day 2: before morning dose of AZD8931
- Cycle 3 Day 2: before morning dose of AZD8931

All samples were processed at the clinical trial site. At each time point, 8mL whole blood was withdrawn from the patient and collected into 2 x4mL Vacutainer® CPT tubes (sodium citrate) and mixed gently. Within 30 minutes (min) of blood draw, samples were centrifuged at 1500g for 20 min at room temperature. The fluffy mononuclear layer at the interface of the two layers was removed using a Pasteur pipette and transferred to a 15 mL Falcon tube. 10 mL cold RPMI 1640 media was added and the tube gently inverted and centrifuged immediately at 200g for 5 min at 4°C. The supernatant was discarded and the cell pellet resuspended in 2 mL freezing mixture (foetal calf serum (FCS) containing 10% dimethylsulphoxide (DMSO)) maintained at 4°C. 1 mL cell suspension was then aliquoted into two labelled cryovials and frozen at -70°C or below.

All samples were analysed for DNA strand breaks using the single cell gel electrophoresis (Comet) assay (Hartley, Spanswick, & Hartley, 2011). All procedures were carried out on ice and in subdued lighting. Samples were thawed on ice, diluted to 2.5 $x10^4$/ml. After embedding cells in 1% agarose on a precoated microscope slide, the cells were lysed for 1hr in lysis buffer (100 mM disodium EDTA, 2.5 M NaCl, 10 mM Tris-HCl pH 10.5) containing 1% Triton X-100 added immediately before analysis, and then washed every 15 min in distilled water for 1hr. Slides were then incubated in alkali buffer (50mM NaOH, 1mM disodium EDTA, pH12.5) for 45 min followed by electrophoresis in the same buffer for 25min at 18 V (0.6V/cm), 250mA. The slides were finally rinsed in neutralising buffer (0.5 M Tris-HCl, pH 7.5) then phosphate buffered saline. After drying the slides were stained with propidium iodide (2.5 µg/mL) for 30 min then rinsed in distilled water. The slides were then dried and stored in a lightproof box until analysis.

Data Analysis and Interpretation: Single cell gel electrophoresis (Comet) Assay

Images were visualised using an Olympus BX51 inverted microscope with a super high pressure Olympus U-RFL-T mercury lamp using a 580 nm dichroic mirror, 535 nm excitation

filter and 645 nm emission filter for propidium iodide staining. The images were captured using a Sony XCD-X710 digital camera and analysed using Komet Analysis software version 5.5 (Andor Technology, UK). For each duplicate slide 25 cells were analysed. The tail moment for each image was calculated using the Komet Analysis software as the product of the percentage DNA in the comet tail and the distance between the means of the head and tail distributions, based on the definition of Olive et al (1990) (Olive, Banath, & Durand, 1990). The greater the Olive tail moment, the greater the level of DNA Damage.

REFERENCES

Barber, P. R., Tullis, I. D. C., Pierce, G. P., Newman, R. G., Prentice, J., Rowley, M. I., Vojnovic, B. (2013). The gray institute “open” high-content, fluorescence lifetime microscopes. *Journal of Microscopy*, *251*(2), 154–167. https://doi.org/10.1111/jmi.12057

Barber, Paul R., Ameer-Beg, S. M., Gilbey, J. D., Edens, R. J., Ezike, I., & Vojnovic, B. (2005). Global and pixel kinetic data analysis for FRET detection by multi-photon time-domain FLIM. In *Multiphoton Microscopy in the Biomedical Sciences V* (Vol. 5700, p. 171). SPIE. https://doi.org/10.1117/12.590510

Hartley, J. M., Spanswick, V. J., & Hartley, J. A. (2011). Measurement of DNA Damage in Individual Cells Using the Single Cell Gel Electrophoresis (Comet) Assay. In *Methods in molecular biology (Clifton, N.J.)* (Vol. 731, pp. 309–320). Methods Mol Biol. https://doi.org/10.1007/978-1-61779-080-5_25

Monypenny, J., Milewicz, H., Flores-Borja, F., Weitsman, G., Cheung, A., Chowdhury, R., … Ng, T. (2018). ALIX Regulates Tumor-Mediated Immunosuppression by Controlling EGFR Activity and PD-L1 Presentation. *Cell Reports*, *24*(3), 630–641. https://doi.org/10.1016/j.celrep.2018.06.066

Olive, P. L., Banath, J. P., & Durand, R. E. (1990). Heterogeneity in radiation-induced DNA damage and repair in tumor and normal cells measured using the “comet” assay. *Radiation Research*, *122*(1), 86–94. https://doi.org/10.2307/3577587

SUPPLEMENTARY FIGURES

Supplementary Figure 1A: Overall survival amongst patients who received AZD (phase I and II) versus patients who received FOLFIRI alone (phase II) - HR: 0.23 (95%CI: 0.06 to 0.84), p=0.03

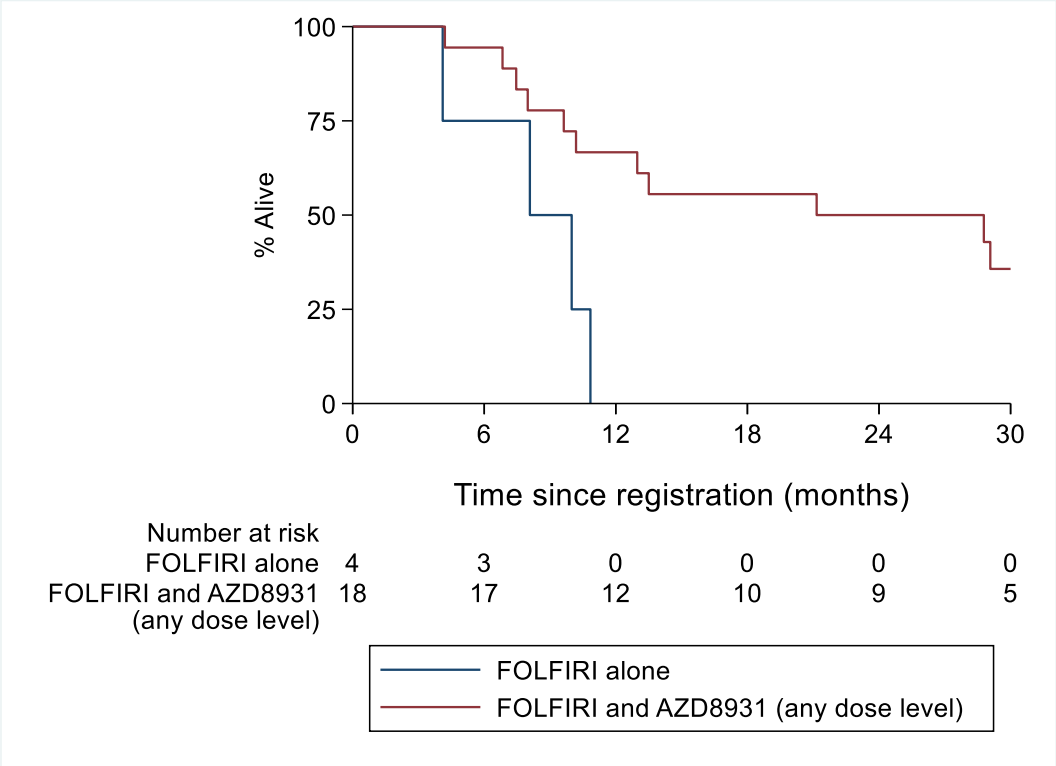

Supplementary Figure 1B: Progression-free survival amongst patients who received AZD (phase I and II) versus patients who received FOLFIRI alone (phase II) - 0.81 (95%CI: 0.27 to 2.49), p=0.72

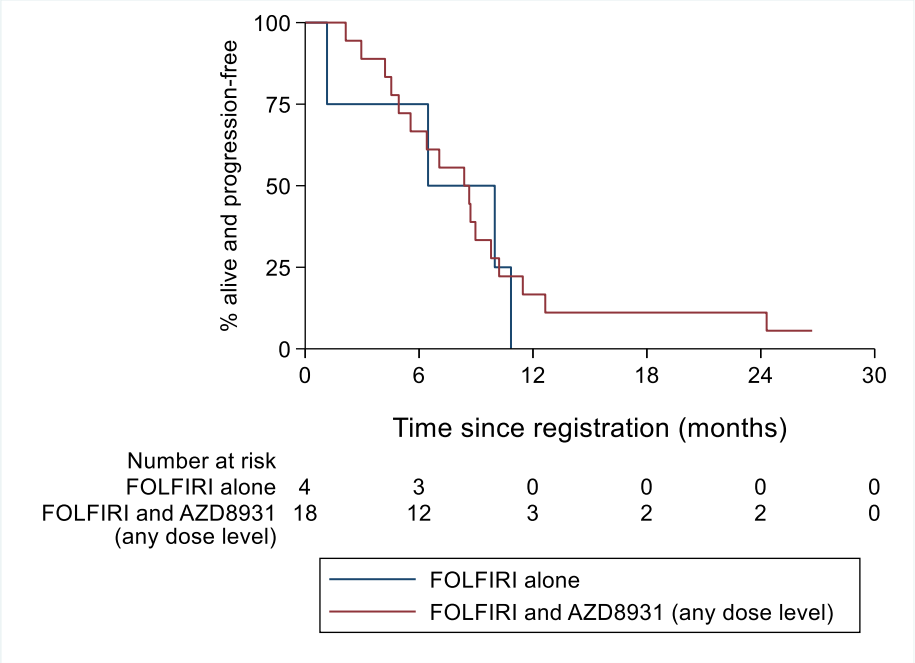

Supplementary Figure 2: Effect of AZD8931 on single strand break DNA damage in PBMCs. The mean olive tail moment (OTM) was calculated for each patient and time point (where available) and grouped per AZD8931 dose (bolus dose, bd day 1-4) cohort: - 20, 40, 80 and 160mg. The greater the OTM, the greater the level of DNA Damage. No significant difference was observed in DNA damage as measured as OTM (μm) between patient dose cohorts of AZD8931 (Figure 1). The level of DNA damage observed across timepoints is considered to be comparable to assay background and no DNA damage was observed in the form of single strand break damage. No inhibition of repair was observed due to lack of initial DNA damage.

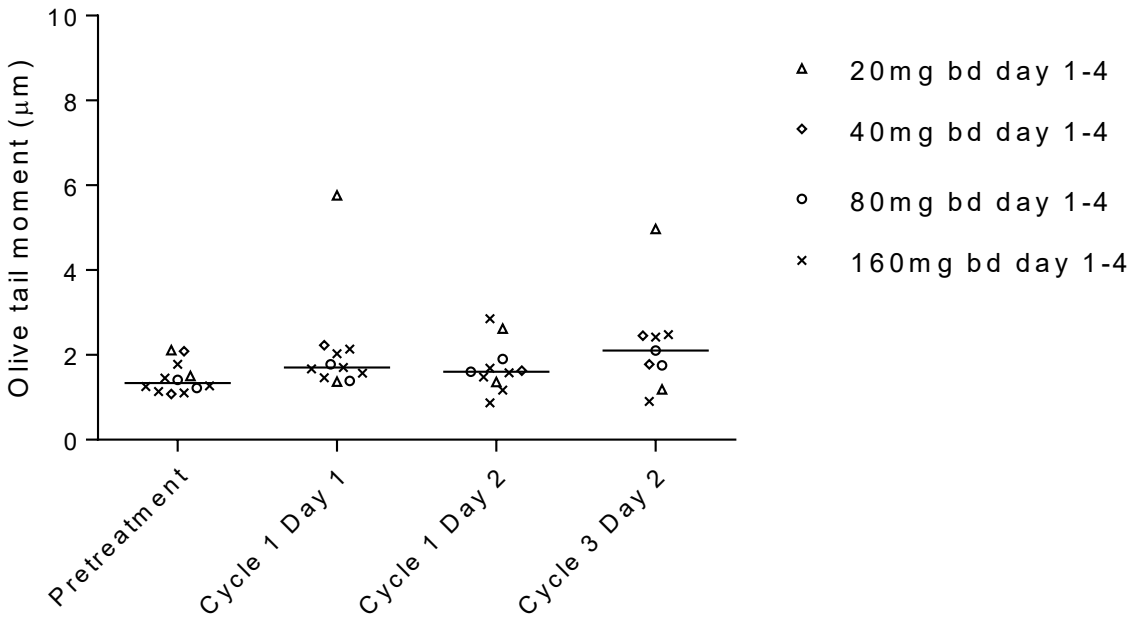

Supplementary Figure 3: Effect of AZD8931 on exosomal proteins. 200-500µl of plasma were used to extract exosomes at 4 different time points per patient (T1-13), before and after first dose of AZD8931; and 5-7 days later, before and after first cycle of chemotherapy combined with AZD8931. Exosome pellets were resuspended in 20-50µl of PBS. Exosome numbers and quality were examined using Nanosight analysis. 5µl/dot were used for protein analysis. There was insufficient plasma for dot blotting at T11.3 for all protein markers, and T13.3 for ALIX. There were no samples received for T12.3 or T12.4.

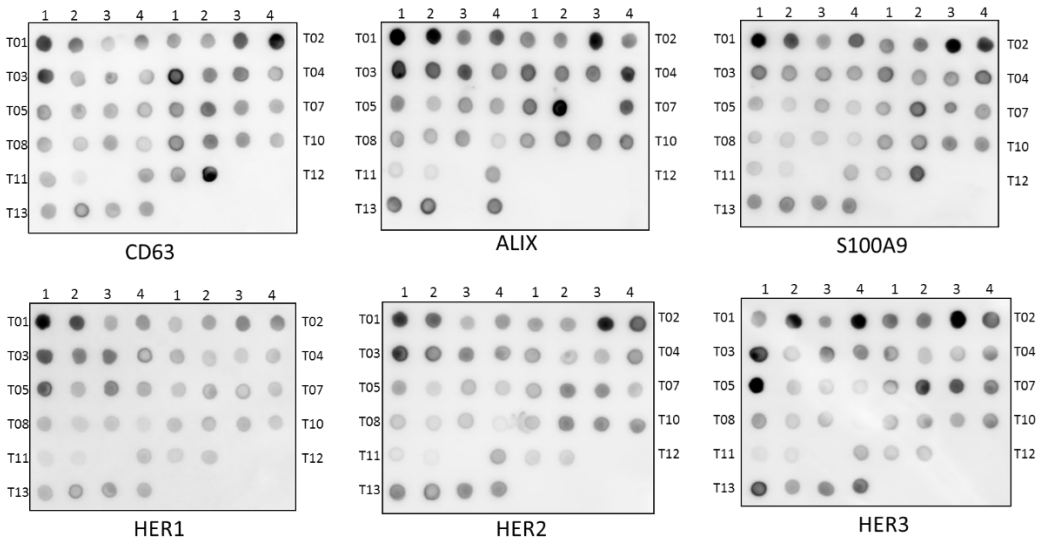

Supplementary Figure 4: Raw HER13 and HER23 FRET dimer scores for all patients before and after first dose of AZD8931. Exosomes were attached to glass slides, blocked with 2 % BSA solution in PBS and stained with anti-EGFR-IgG-Alexa Fluor546 (Cetuximab) and anti-ErbB3-IgG-Cy5 (clone REA508, Miltenyi Ltd.) ON at 4 °C. The excess of antibodies was removed by washing with PBS, stained exosomes were the covered with thio-diethanol as a mounting media. The degree of dimerization was quantified with FLIM/FRET. Custom time-domain fluorescence lifetime 'Open' microscopes 'Hooke' and 'Galileo' were used to image exosome slides with a Nikon 20x Plan Fluor objective lens (0.5 NA) as previously described (P. R. Barber et al., 2013). FLIM images of the donor channel were obtained through a filter set optimized for use with Alexa546 (Semrock filters FF01-540/15-25, NT48-492 30R/70T, FF01-593/40-25). Widefield images of the donor channel were acquired through a 'Cy3' cube (Ex: 510-560 nm, Em: 573-648 nm) and of the acceptor channel through a 'Cy5' cube (Ex: 590-650 nm, Em: 663-738 nm). Slides were imaged with a laser power and scan speed to gain sufficient photon counts within 5 minutes of imaging (typically >100 photon counts per pixel peak). Image dimensions were 256x256 pixels (328x328 microns) by 256 time-resolved bins (spanning 15.0 ns). Optical resolution is approximately 1 micron. Individual exosomes are not resolved but appear as diffraction limited spots. Typically, several thousand exosomes are imaged per field of view, occupying on the order of 10 % of the image pixels. FLIM lifetime measurements were performed with the TRI2 software (version 2.7.8.9, Gray Institute, Oxford) as described previously (Paul R. Barber et al., 2005). Briefly, exosomes were isolated from the background using a threshold that was set by measuring the mode and standard deviation (SD) of the background (based on the modal image intensity and left-hand tail or estimated from Poisson statistics for mode <10 photon counts). The threshold was then set at (mode + 6xSD). This excluded all background-only pixels and aims to ensure sufficient exosome signal in the remainder (since exosome size << 1 pixel, the sample-derived background signal is not displaced by exosome presence, see supplementary exosome intensity modelling). The pixels above the threshold in one field of view were binned into a single transient signal. This transient was fitted with a tri-exponential model of the form: $I = z + A_1 e^{-t/\tau_1} + A_2 e^{-t/\tau_2} + A_3 e^{-t/\tau_3}$. Where I represents signal intensity, z represents a constant background, A represents signal component amplitudes, t represents time and tau the fitted fluorescence characteristic lifetimes. Two lifetimes, τ_2 and τ_3, were held constant throughout the analysis at 0.3 ns and 1.0 ns (determined empirically from background test samples) to capture autofluorescence and other interfering components, as previously described, away from the target Alexa546 lifetime of circa 2.5 ns. These components are held constant, and not allowed to vary, to improve fit stability. The value of the free lifetime, τ_1, was used to represent the lifetime of Alexa546 in the field of view. Between 3 and 5, D and DA

sample regions were imaged per patient. Lifetimes for D and DA were averaged (giving τ_D and τ_{DA}) from the region lifetimes, and a FRET value for the patient was calculated by: $FRET=1-\frac{\tau_{DA}}{\tau_D}$.

FRET score was classified as positive or negative according to whether a significant dimer score could be detected for that patient time point, as follows. Five FLIM images with the FRET pair along with five control images were acquired per time point. Images were quality controlled to remove large particles and clumps (> around 500 um) by manual masking. The FRET standard error in the mean (SEM) was calculated from the FRET and control samples, and FRET was classed as positive if the mean value was positive and the SEM did not cross below the zero line.

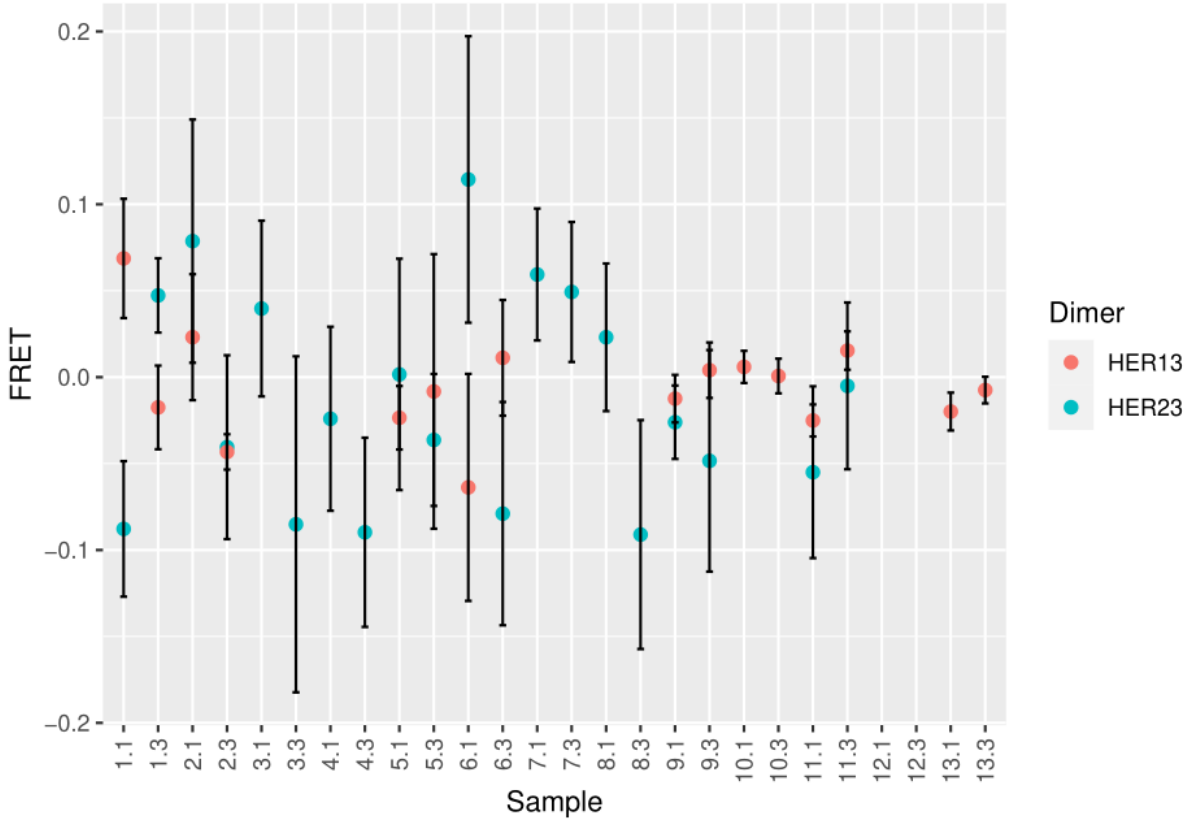

Supplementary Figure 5: Changes in HER2-3 dimerisation in colorectal cells upon treatment with AZD8931.

A) LIM1215 cells were plated on coverslips and treated with either cetuximab (15µg/ml or 100nM) or AZD8931 (10µM) for 1 hour, prior to fixation with 4% PFA, and staining with IgG anti-HER2-Cy5 (acceptor) and IgG anti-HER3-Alexa546 (donor). D: Donor alone; DA: Donor with acceptor. Averaged FRET values were calculated on a pixel-by-pixel basis, and the distribution of pixelwise FRET efficiencies plotted for each condition tested. B) Increased HER2-3 dimerisation in LIM1215 with cetuximab and AZD8931. Using paired T-test, p=*0*.043 for cetuximab vs control, *p*=0.003 for AZD8931 vs control. C) Reduced HER2:HER3 dimerisation in DLD1 (KRAS WT) upon AZD8931. *p*=0.077 for cetuximab vs control, *p*=0.026 for AZD8931 vs control. Results are representative of 5 technical repeats each from 2 independent experiments.

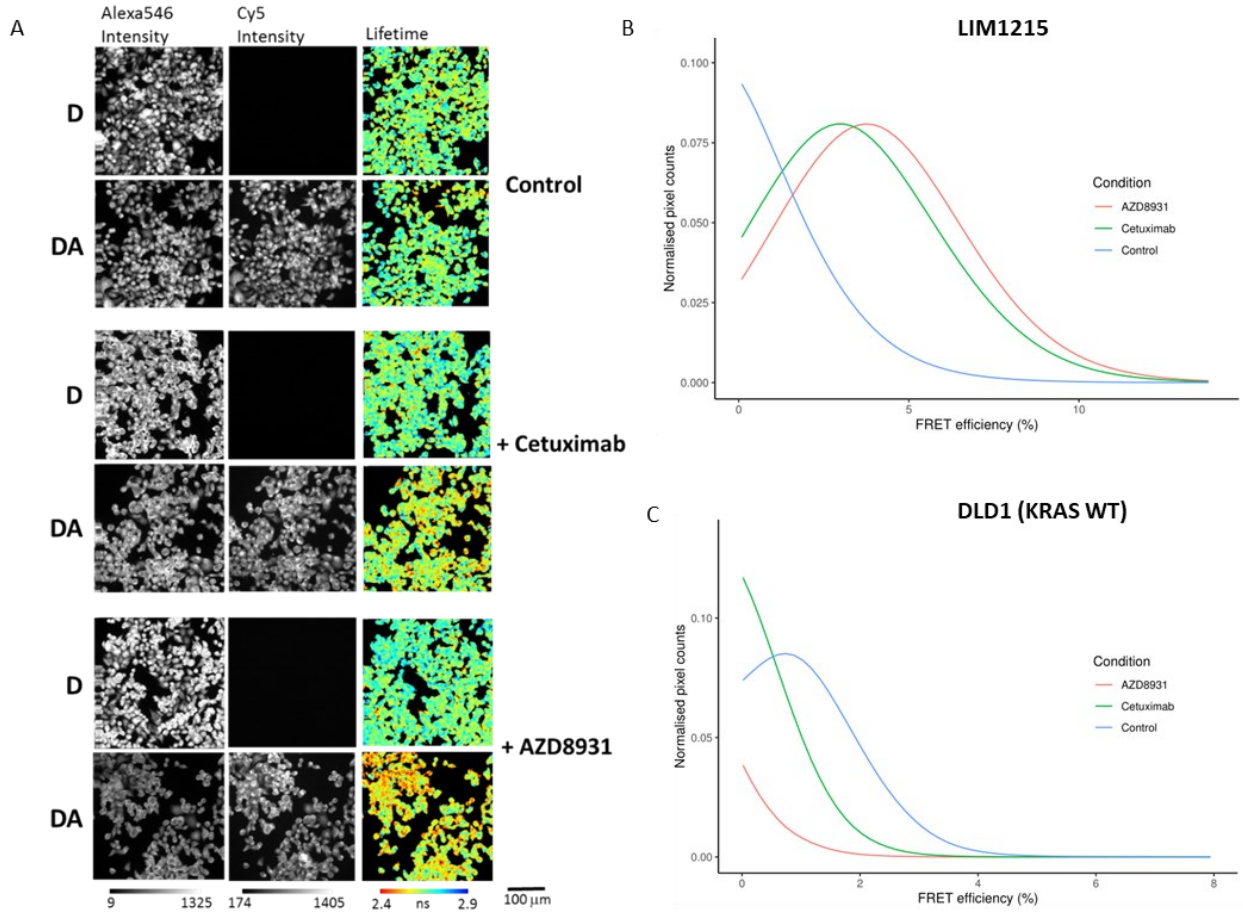

Corresponding Author Name: Prof Daniel Hochhauer
Manuscript Number: BJC-A3340844R-A

Reporting Summary

Springer Nature wishes to improve the reproducibility of the work that we publish. This checklist is used to ensure good
reporting standards and to improve the reproducibility. Please respond completely to all questions relevant to your
manuscript. For more information, please read the journal's Guide to Authors.

✓☐ **Check here to confirm that the following information is available in the Material & Methods section:**

- **The exact sample size (*n*)** for each experimental group/condition, given as a number, not a range
- **A description of the sample collection** allowing the reader to understand whether the samples represent technical or biological replicates (including how many animals, litters, culture, etc.)
- **A statement of how many times the experiment shown was replicated in the laboratory**
- **Definitions of statistical methods and measures**: For small sample sizes (n<5) descriptive statistics are not appropriate, instead plot individual data points
  - Very common tests, such as *t*-test, simple χ_2 tests, Wilcoxon and Mann-Whitney tests, can be unambiguously identified by name only, but more complex techniques should be described in the methods section
  - Are tests one-sided or two-sided?
  - Are there adjustments for multiple comparisons?
  - **Statistical test results**, e.g., ***P* values**
  - Definition of **'center values'** as **median or mean**;
  - Definition of **error bars as s.d. or s.e.m. or c.i.**

Please ensure that the answers to the following questions are reported in the manuscript itself. We encourage you to include a specific subsection in the methods section for statistics, reagents and animal models. Below, provide the page number or section and paragraph number.

Statistics and general methods	**Reported in section/paragraph or page #**
1. How was the sample size chosen to ensure adequate power to detect a pre-specified effect size? (Give section/paragraph or page #)	Methods - Participants and study design Page 5, lines 135-147
For animal studies, include a statement about sample size estimate even if no statistical methods were used.	N/A
2. Describe inclusion/exclusion criteria if samples or animals were excluded from the analysis. Were the criteria pre-established? (Give section/paragraph or page #)	N/A
3. If a method of randomization was used to determine how samples/animals were allocated to experimental groups and processed, describe it. (Give section/paragraph or page #)	N/A
For animal studies, include a statement about randomization even if no randomization was used.	N/A
4. If the investigator was blinded to the group allocation during the experiment and/or when assessing the outcome, state the extent of blinding. (Give section/paragraph or page #)	N/A
For animal studies, include a statement about blinding even if no blinding was done.	N/A
5. For every figure, are statistical tests justified as appropriate?	N/A, the main analysis is descriptive; treatment comparisons in terms of OS and PFS were reported using hazard ratios, 95%CI and p-values (2-

	sided) derived from cox regression (Methods – Data Analysis, page 6, lines 178-184)
Do the data meet the assumptions of the tests (e.g., normal distribution)?	N/A, the analysis is descriptive; plots are presented.
Is there an estimate of variation within each group of data?	N/A, results are reported using confidence intervals (Methods – Data Analysis, page 6, lines 178-184)
Is the variance similar between the groups that are being statistically compared? (Give section/paragraph or page #)	This is a single arm study. (Results – Time to event outcome, page 8, lines 244-247 presents a secondary analysis where AZD patients are compared statistically to FOLFORI alone patients in terms of OS and PFS)
Reagents	**Reported in section/paragraph or page #**
6. Report the source of antibodies (vendor and catalog number)	N/A
7. Identify the source of cell lines and report if they were recently authenticated (e.g., by STR profiling) and tested for mycoplasma contamination	N/A
Animal Models	**Reported in section/paragraph or page #**
8. Report species, strain, sex and age of animals	N/A
9. For experiments involving live vertebrates, include a statement of compliance with ethical regulations and identify the committee(s) approving the experiments.	N/A
Human subjects	**Reported in section/paragraph or page #**
11. Identify the committee(s) approving the study protocol.	Additional information - Ethics approval and consent to participate Page 12
12. Include a statement confirming that informed consent was obtained from all subjects.	Additional information - Ethics approval and consent to participate Page 12
13. For publication of patient photos, include a statement confirming that consent to publish was obtained.	N/A
14. Report the clinical trial registration number (at ClinicalTrials.gov or equivalent).	Abstract Page 2
Data deposition	**Reported in section/paragraph or page #**
17. Provide accession codes for deposited data. Data deposition in a public repository is mandatory for: a. Protein, DNA and RNA sequences b. Macromolecular structures c. Crystallographic data for small molecules d. Microarray data	N/A
18. If computer code was used to generate results that are central to the paper's conclusions, include a statement in the Methods section under "**Code availability"** to indicate whether and how the code can be accessed. Include version information as necessary and any restrictions on availability.	Methods - Code availability Page 7, Lines 189-190

CONSORT 2010 checklist of information to include when reporting a randomised trial*

Section/Topic	Item No	Checklist item	Reported on page No
Title and abstract			
	1a	Identification as a randomised trial in the title	
	1b	Structured summary of trial design, methods, results, and conclusions (for specific guidance see CONSORT for abstracts)	2
Introduction			
Background and objectives	2a	Scientific background and explanation of rationale	3-4
	2b	Specific objectives or hypotheses	5
Methods			
Trial design	3a	Description of trial design (such as parallel, factorial) including allocation ratio	5
	3b	Important changes to methods after trial commencement (such as eligibility criteria), with reasons	6
Participants	4a	Eligibility criteria for participants	5
	4b	Settings and locations where the data were collected	6
Interventions	5	The interventions for each group with sufficient details to allow replication, including how and when they were actually administered	5-7
Outcomes	6a	Completely defined pre-specified primary and secondary outcome measures, including how and when they were assessed	5-6
	6b	Any changes to trial outcomes after the trial commenced, with reasons	N/A
Sample size	7a	How sample size was determined	5-6
	7b	When applicable, explanation of any interim analyses and stopping guidelines	N/A
Randomisation:			
Sequence generation	8a	Method used to generate the random allocation sequence	
	8b	Type of randomisation; details of any restriction (such as blocking and block size)	
Allocation concealment mechanism	9	Mechanism used to implement the random allocation sequence (such as sequentially numbered containers), describing any steps taken to conceal the sequence until interventions were assigned	
Implementation	10	Who generated the random allocation sequence, who enrolled participants, and who assigned participants to interventions	
Blinding	11a	If done, who was blinded after assignment to interventions (for example, participants, care providers, those	N/A

		assessing outcomes) and how	
	11b	If relevant, description of the similarity of interventions	N/A
Statistical methods	12a	Statistical methods used to compare groups for primary and secondary outcomes	6
	12b	Methods for additional analyses, such as subgroup analyses and adjusted analyses	6
Results			
Participant flow (a diagram is strongly recommended)	13a	For each group, the numbers of participants who were randomly assigned, received intended treatment, and were analysed for the primary outcome	6-7
	13b	For each group, losses and exclusions after randomisation, together with reasons	6-7, Figure 1
Recruitment	14a	Dates defining the periods of recruitment and follow-up	7
	14b	Why the trial ended or was stopped	7
Baseline data	15	A table showing baseline demographic and clinical characteristics for each group	Table 1
Numbers analysed	16	For each group, number of participants (denominator) included in each analysis and whether the analysis was by original assigned groups	6-8, Figure 1
Outcomes and estimation	17a	For each primary and secondary outcome, results for each group, and the estimated effect size and its precision (such as 95% confidence interval)	7-8
	17b	For binary outcomes, presentation of both absolute and relative effect sizes is recommended	N/A
Ancillary analyses	18	Results of any other analyses performed, including subgroup analyses and adjusted analyses, distinguishing pre-specified from exploratory	8-9
Harms	19	All important harms or unintended effects in each group (for specific guidance see CONSORT for harms)	7
Discussion			
Limitations	20	Trial limitations, addressing sources of potential bias, imprecision, and, if relevant, multiplicity of analyses	9-11
Generalisability	21	Generalisability (external validity, applicability) of the trial findings	9-11
Interpretation	22	Interpretation consistent with results, balancing benefits and harms, and considering other relevant evidence	9-11
Other information			
Registration	23	Registration number and name of trial registry	2 (abstract)
Protocol	24	Where the full trial protocol can be accessed, if available	
Funding	25	Sources of funding and other support (such as supply of drugs), role of funders	13

*We strongly recommend reading this statement in conjunction with the CONSORT 2010 Explanation and Elaboration for important clarifications on all the items. If relevant, we also recommend reading CONSORT extensions for cluster randomised trials, non-inferiority and equivalence trials, non-pharmacological treatments, herbal interventions, and pragmatic trials. Additional extensions are forthcoming: for those and for up to date references relevant to this checklist, see www.consort-statement.org.